SMHI RMK
Nr 57, August 1988

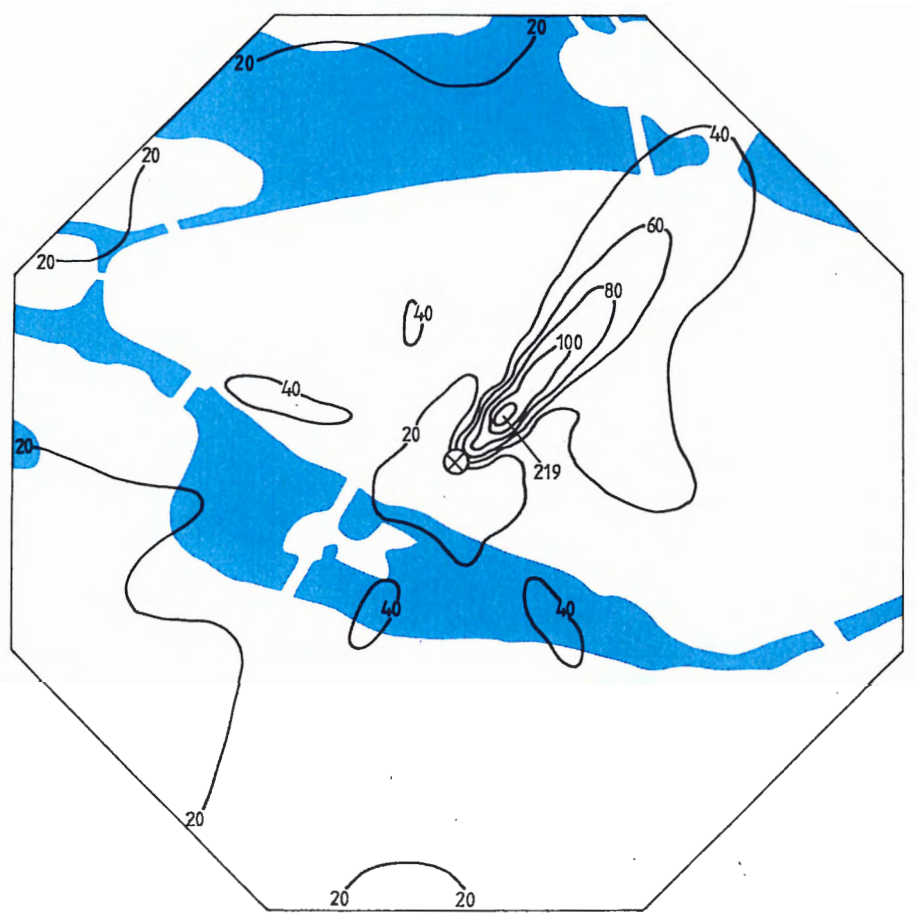

AN OPERATIONAL AIR POLLUTION MODEL

by Gunnar Omstedt

SMHI REPORTS
METEOROLOGY and CLIMATOLOGY

Nr 57, August 1988

AN OPERATIONAL AIR POLLUTION MODEL

by Gunnar Omstedt

SMHIs tryckeri, Norrköping 1988.

Issuing Agency

SMHI
S-601 76 NORRKÖPING
Sweden

Report number

RMK 57

Report date

Augusti 1988

Author (s)

Gunnar Omstedt

Title (and Subtitle)

AN OPERATIONAL AIR POLLUTION MODEL

Abstract

This report describes an operational air pollution model developed at the Swedish Meteorological and Hydrological Institut for the prediction of air pollution concentrations on a local scale. Predictions can be made in one or several receptor points for emissions from point, area- and traffic sources. The model is partly based on the Danish so called OML-model (Berkowicz et al., 1985).

Key words

Operational air pollution model, Gaussian plume model, air pollution forecast

Supplementary notes

Number of pages

28

Language

English

ISSN and title

0347-2116 SMHI Reports Meteorology and Climatology

Report available from:

Liber Grafiska AB-Förlagsorder
S-162 89 STOCKHOLM
Sweden

AN OPERATIONAL AIR POLLUTION MODEL

LIST OF CONTENTS

1. Introduction

In this report an operational air pollution model developed at the Swedish Meteorological and Hydrological Institute (SMHI) will be described. It predicts air pollution concentrations on a local scale, i.e. a length scale of about 10 km. A schematic picture of the model, called LSAM, is given in figure 1.

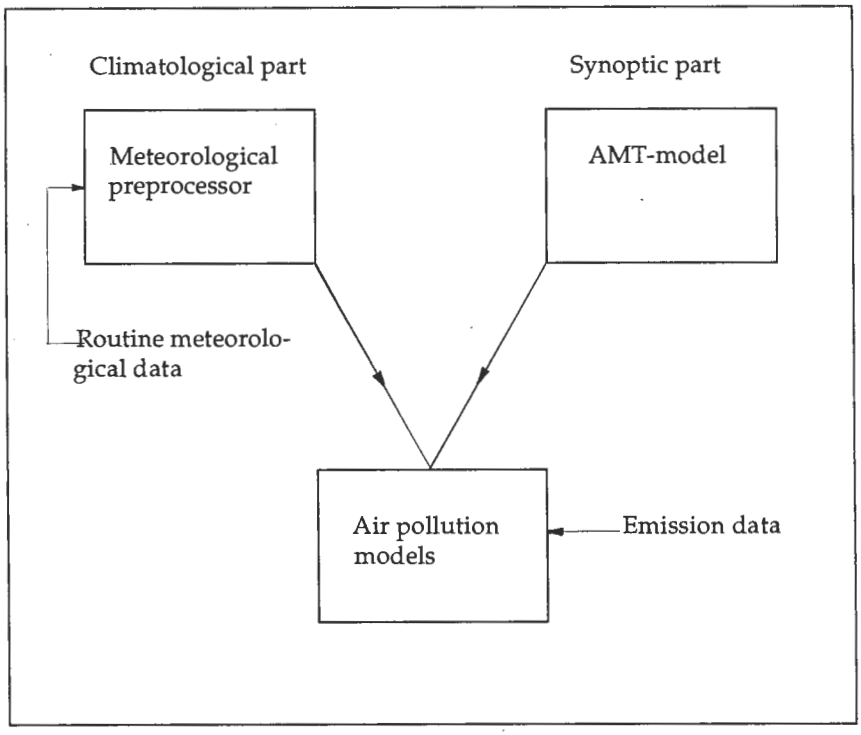

Figure 1. A schematic picture of the Local Scale Air pollution Model (LSAM) used at SMHI.

Prediction of air pollution concentrations can be made in two different ways:

1. Climatologically, in which concentrations are calculated hourly on the basis of long-term time series of input data. For this purpose a so called "meteorological preprocessor" is used for calculation of atmospheric boundary layer parameters by using routine meteorological data.

2. Synoptically, in which hourly concentrations are calculated from real-time or forecast input data. For this purpose a so called Air-Mass-Transformation model is used.

The model is limited to dry atmospheric boundary layers (i.e. to boundary layers in which no significant amount of clouds or fog are present) and to reasonably flat terrain. It is partly based on the Danish so called OML-model, which has been tested on non-buoyant plumes from tracer experiments as well as on buoyant plumes from power plants with good results (Berkowicz et al., 1985).

2. Atmospheric boundary layer parameters

The physical basis for the meteorological parts of the model is provided by parameterizations of the structure of the atmospheric boundary layer (ABL) and its interaction with the ground. The conditions in the ABL are described by three primary atmospheric boundary layer parameters i.e. the atmospheric boundary layer height, the sensible heat flux and the friction velocity. These parameters determine a number of secondary parameters. A brief listing of parameters used in the model - their definition and physical meaning - is given below.

The atmospheric boundary layer height, h, is defined as the depth of the turbulent boundary layer. The lower part of it, where the fluxes of momentum and heat are approximately constant with height, is called the surface layer. The depth of the surface layer is denoted by, h_{sl}.

The surface sensible heat flux, H, is the value at the surface of the vertical flux of sensible heat that is transfered by turbulence from or to the surface. It determines the heating or cooling of the ABL. Due to the action of gravity, the heat flux gives rise to buoyant production or destruction of turbulent kinetic energy. This production is given by

$$H_* = \frac{gH}{\rho C_p T} \qquad (2.1)$$

where g is the acceleration of gravity, ρ the air density, C_p the specific heat of air at constant pressure and T the air temperature. When H is positive turbulence is created by buoyancy. In this case H_* and h define the convective velocity scale

$$w_* = (H_* h)^{1/3} \qquad (2.2)$$

which is the turbulent velocity scale in the unstable ABL.

The surface momentum flux, τ, defines the friction velocity

$$u_* = (\tau/\rho)^{1/2} \qquad (2.3)$$

where u_* determines the shear production of turbulent kinetic energy at the surface.

The surface sensible heat flux and the friction velocity define a temperature scale:

$$\theta_* = \frac{-H}{\rho C_p u_*} \qquad (2.4)$$

which is a temperature scale for the turbulent heat transfer.

The friction velocity and the temperature scale, θ_*, define the Obukov length scale

$$L = \frac{u_*^2}{(kg\theta_*/T)} \qquad (2.5)$$

where k is the von Karman constant.

Other important length scales are the surface roughness length, z_o, and the height above the surface, z.

An outline for a "meteorological preprocessor" similar to the one presented here is given by van Ulden and Holtslag (1985).

2.1 A meteorological preprocessor

A meteorological preprocessor for climatological calculations of atmospheric boundary layer parameters has been developed. The preprocessor has been used to form a meteorological data bank of atmospheric boundary layer parameters for about 30 different places in Sweden where hourly routine meteorological data and data from radio soundings for about 4 years have been used (Bäckström et al.,1984). A summary of the methods used is given in sec. 2.2-2.4 below.

2.2 Surface fluxes

The starting point is the equation for the surface energy balance

$$Rn = LE + H + G \qquad (2.2.1)$$

where Rn is the net radiation, LE the latent heat flux, H the sensible heat flux and G the soil heat flux.

The net radiation is the balance between downward and upward short-wave and long-wave radiations. Nielsen et al.(1981) have developed methods for estimation of net radiation by using routine meteorological data such as cloud cover and types, temperature and wind speed. The methods have been tested against 10 years of data in Denmark with good results (Nielsen et al.,1981) and compared with six days of data at a site in Sweden (Klockrike) with another surface albedo. The agreement for this small time period was also good. These methods are followed.
In order to estimate the other three terms of (2.2.1) a method developed by Berkowicz and Prahm (1982) is used. The latent heat is calculated by the Penman-Monteith equation.

$$LE = \frac{(Rn-G)r_a(\Delta/\gamma)+Dq\rho C_p/\gamma}{r_s+(1+(\Delta/\gamma))r_a} \qquad (2.2.2)$$

where Δ is the gradient of the saturated vapour pressure with respect to temperature and γ is the psychrometric constant.

Dq is the humidity deficit in air defined by

$$Dq = q_s(T)-q \qquad (2.2.3)$$

where $q_s(T)$ is the saturated vapour pressure at the temperature T and q is the actual vapour pressure.

The aerodynamic resistance, r_a, is the so called resistance of the atmosphere for water vapour transfer between a given height level and the surface. It is expressed in terms of known flux profile relationships based on Monin-Obukhov's similarity theory.

The surface resistance, r_s, is the resistance of the surface to water vapour transport. It is related to the humidity deficit in the air, Dq, by the following equation

$$r_s = (Dq/F)(\rho C_p/\gamma) \qquad (2.2.4)$$

where F is an empirical function of the surface moisture conditions.

The soil heat flux G is modelled as a certain fraction of the sensible heat flux

$$G = \alpha_g H \qquad (2.2.5)$$

where α_g is a constant with a typical value of 0.3 for a grass covered surface.

The sensible heat flux can now be calculated from (2.2.1),(2.2.2) and (2.2.5) by the following equation:

$$H = \frac{Rn(r_a+r_s)-Dq(\rho C_p/\gamma)}{r_s+(1+\Delta/\gamma)r_a+\alpha_g(r_a+r_s)} \qquad (2.2.6)$$

This equation is solved by an iteration method given as outputs sensible heat flux, friction velocity and Obukhov length scale.

The surface energy balance method, was compared with experimental data from three sites in Denmark (Hojbakke-gaard), Sweden (Marsta) and Holland (Cabauw) with good results (Berkowicz and Prahm, 1982).

	Stability Classes (Obukhov length scale (m))								
Wind direction	a	b	c	d	e	f	g	h	i
10	5	5	6	51	45	25	12	24	50
20	2	8	11	31	35	22	9	32	35
30	8	2	11	35	57	28	21	31	39
40	1	10	11	12	31	17	10	22	35
50	3	8	5	14	21	6	8	21	45
60	12	14	14	18	45	14	8	20	46
70	9	12	19	21	28	11	5	10	13
80	5	15	17	12	30	7	4	8	12
90	15	11	11	10	18	8	4	12	28
100	6	16	8	9	16	5	4	3	15
110	5	16	12	28	18	8	6	12	9
120	13	19	18	58	44	14	7	11	31
130	12	12	19	61	34	12	6	18	41
140	9	14	21	56	24	16	13	22	50
150	4	11	28	48	48	25	12	50	111
160	5	9	18	38	45	22	5	25	74
170	6	9	10	34	35	18	16	34	48
180	6	9	9	56	39	24	9	30	60
190	11	13	16	50	55	19	13	27	55
200	14	20	26	50	67	25	13	50	73
210	9	24	30	35	55	41	22	73	144
220	0	19	21	24	41	18	12	42	82
230	6	16	13	23	52	23	13	41	101
240	10	20	28	49	73	38	17	49	86
250	2	16	26	83	64	38	10	41	65
260	2	20	39	64	53	26	13	33	55
270	10	19	31	61	96	25	11	39	76
280	7	19	17	38	53	18	14	49	52
290	6	12	15	37	41	26	10	26	107
300	6	18	7	54	77	23	27	41	43
310	8	8	12	37	74	30	11	45	61
320	2	5	8	30	69	22	10	19	61
330	4	4	15	68	65	28	12	42	72
340	3	8	14	53	71	33	10	34	44
350	5	5	23	55	46	22	12	29	35
360	2	9	20	69	45	23	10	37	65
Number of hours:	233	455	609	1472	1710	760	399	1102	2019

Unstable = 14.8 (%)
Neutral = 16.8 (%)
Stable = 68.4 (%)

a: -40<L<0, b: -200<L<-40, c: -1000<L<-200
d: |L|>1000
e: 200<L<1000, f: 100<L<200, g: 40<L<100, h: 10<L<40, i: 0<L<10

TABLE 1. A frequency table (number of hours) for atmospheric stability (defined by the Obukhov length scale) and wind direction for Bromma in Sweden 1981.

Examples of model outputs are given in table 1. The table gives information on the frequency of occurence of different stability classes, as defined by Obukhov length scale, at one place in Sweden (Bromma) for the year 1981.

2.3 The atmospheric boundary layer height

The atmospheric boundary layer height or, as it is often called, the mixing height, is calculated for unstable, neutral and stable meteorological conditions.

The unstable atmospheric boundary layer shows over land a strong day-time development. It is often capped by an inversion. As the boundary layer heats up during the course of a sunny day, the inversion base gradually rises because the turbulence in the boundary layer entrains the warmer air above the inversion base. Within the boundary layer and above 0.1h the vertical profile of potential temperature is relatively uniform. In the inversion layer potential temperature rapidly increases with height to the value in the overlying non-turbulent stable air. In figure 2 a schematic picture of these observations is shown.

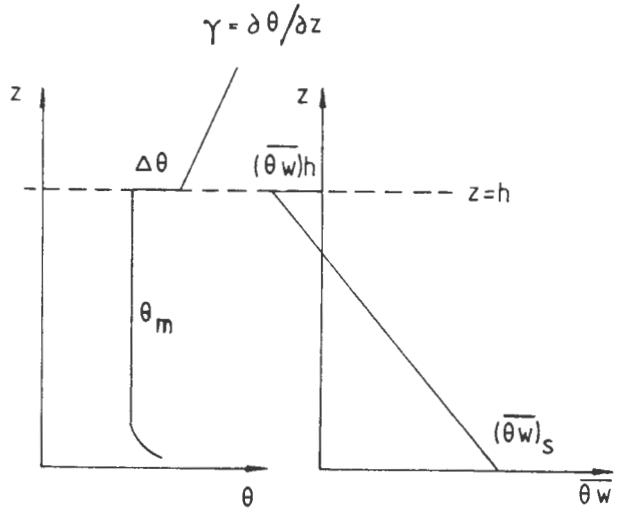

Figure 2. A schematic picture of the vertical distributions of potential temperature and turbulent heat flux in and above an unstable atmospheric boundary layer.

The inversion layer is considered thin enough to be represented by a discontinuity, $\Delta\theta$, in potential temperature. Making use of figure 2 the following equations can be derived (Tennekes,1973).

$$\frac{d\theta_m}{dt} = \frac{1}{h}\left(\left(\overline{\theta w}\right)_s - \left(\overline{\theta w}\right)_h\right) \; ; \; \left(\overline{\theta w}\right)_s = \frac{H}{\rho C_p} \qquad (2.3.1)$$

$$\frac{d\Delta\theta}{dt} = \gamma\left(\frac{dh}{dt} - \overline{w}_h\right) - \frac{d\theta_m}{dt} \qquad (2.3.2)$$

$$-\left(\overline{\theta w}\right)_h = \Delta\theta\left(\frac{dh}{dt} - \overline{w}_h\right) \qquad (2.3.3)$$

where θ_m is the mean potential temperature, $\overline{w}_h$ is the large-scale vertical velocity at z=h. The subscripts 's' and 'h' refer to the surface and boundary layer height respectively. The other notations are given in the figure.

In order to obtain solutions to these equations an equation that relates dh/dt to the energetics of the turbulence in the boundary layer is needed. Several such possibilities have been proposed (Tennekes and Driedonks, 1981). By using an extensive set of field data, Driedonks (1982) has shown that good results can be obtained by the following entrainment formulation.

$$-\left(\overline{\theta w}\right)_h = 0.2\left(\overline{\theta w}\right)_s + \frac{5u_*^3 T}{gh} \qquad (2.3.4)$$

Olesen et al. (1985) have combined the above equations with data from radio soundings, neglecting the large-scale vertical velocity. This procedure is followed. The 00 UTC sounding is used to start the integration. The sensible heat flux is calculated by using the surface energy balance method (sec. 2.2). When the sensible heat flux first becomes positive the daytime unstable boundary layer height is calculated hourly by equations (2.3.1-2.3.4). At 12 UTC the sounding from that time is introduced. A comparsion is made between calculated height and observed height, defined as the height to the first stable layer determined from the sounding. If a substantial difference occurs a correction is made for all previous calculated values. The further integration proceeds from the 12 UTC profile. A comparsion is made between the 00 and 12 UTC sounding to ensure that the advection is not too extreme.

When the conditions during daytime do not permit the use of the above model a formula for the neutral boundary layer is used, given by

$$h = 0.25\ u_*/f \qquad (2.3.5)$$

where f is the Coriolis parameter.

Stable boundary layers are complex, showing considerable variability in space and time. Knowledge of them is less well defined than is the case for the unstable boundary layers. Most of the models for the stable boundary layer height are diagnostic, based on steady-state assumption and on dimensional arguments. In reality, however, the stable boundary layer is generally not in a steady-state. Therefore several authors have developed prognostic models which describes the development of the stable boundary layer height as a function of time (see e.g. Nieuwstadt, 1984). However these models introduce new parameters which are not easy to estimate using only routine meteorological data. For climatological calculations we therfore use a diagnostic model suggested by Zilitinkevich (1972).

$$h = c_s (u_* L/f)^{1/2} \qquad (2.3.6)$$

where $c_s \simeq 0.4$ is an empirical coefficient. This model agrees resonably well with observations according to Nieuwstadt (1984). Equation (2.3.6) gives however unrealistic values for large values of L. The stable boundary layer height is therefore limited by its neutral value in cases for which eq. (2.3.6) gives higher values than eq.(2.3.5).

To ensure that plumes will be trapped inside stable boundary layers a lower bound of 150 m is also chosen.

Examples of model outputs are given in figure 3. The figure shows median boundary layer height values (full line) as a function of the (local) time of the day. Four years of routine meteorological data have been used for one place in Sweden (Bromma). Dotted lines shows 80-percentile and 20-percentile boundary layer height values, i.e 60 % of the values are confined between these two lines.

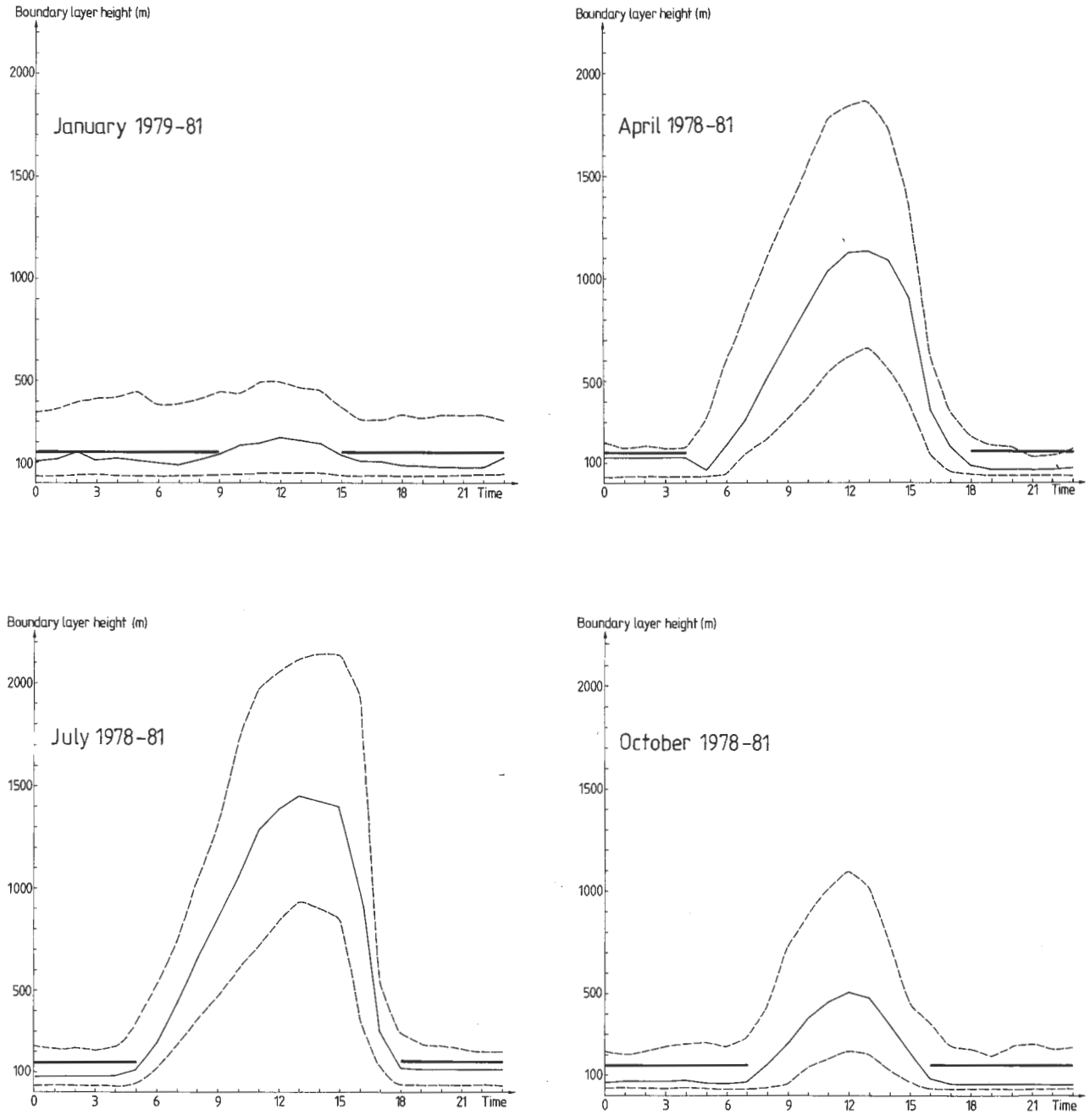

Figure 3. Climatologically calculated atmospheric boundary layer heights as function of the (local) time of the day for Bromma (Sweden) 1978-81. Full line represent median values and dotted lines represents 80-percentile and 20-percentile boundary layer height values. The thick line represent the lower bound of 150 m used in the model for the stable boundary layer height.

2.4 Wind- and temperature profiles

In the lower part of the ABL the wind speed normally increases with height and at the same time turns with height, clockwise in the Northern Hemisphere, as a result of the Coriolis force. The wind turning with height affects both the direction in which pollution travels and the lateral dispersion. Only the first effect is, for the time being, included in the model. The wind turning with height is described in a simple way by following expression:

$$dd(h_e) - dd(z_a) = \alpha \frac{(h_e - z_a)}{(h - z_a)} \qquad (2.4.1)$$

where $dd(h_e)$ is the wind direction at the effective source height, h_e, $dd(z_a)$ is the wind direction at the anemometer level, z_a, and α is a parameter describing the wind directional shear. Here we use a value of α=30 deg. for stable conditions, which roughly fits the data analysed by Holtslag (1984) and α=10 deg. for unstable conditions. The mean wind speed is calculated in the surface layer according to the Monin-Obukhov similarity theory, by the following equation:

$$u(z) = \frac{u_*}{k}\left[\ln(z/z_o) - \Psi_m(z/L) + \Psi_m(z_o/L)\right] \quad \text{when } z \leq h_{s1} \qquad (2.4.2)$$

where z_o is the roughness length, k is the von Karman constant which has been set equal to 0.4, h_{s1} is the surface layer height and Ψ_m is the stability function. Several forms of Ψ_m have been proposed in the literature. Here we follow the results obtained by Holtslag (1984 and 1988) from observations of wind and temperature in the 213 m high meteorological mast in Cabau in the Netherlands. From these studies we select for unstable conditions (L<0) Dyer's (1974) function

$$\Psi_m(z/L) = 2\ln\left(\frac{1+x}{2}\right) + \ln\left(\frac{1+x^2}{2}\right) - 2\tan^{-1}(x) + \pi/2 \qquad (2.4.3)$$

where $x = (1-16z/L)^{1/4}$

and for stable conditions (L>0) a stability function from Holtslag (1988) which gave good results even in very stable conditions

$$-\Psi_m = a\frac{z}{L} + b\left(\frac{z}{L} - \frac{c}{d}\right)\exp\left(-d\frac{z}{L}\right) + \frac{bc}{d} \qquad (2.4.4)$$

where a=0.7 ,b=0.75 ,c=5. and d=0.35.

Above the surface layer the mean wind speed is taken to be constant with the value at h_{s1}.

$$u(z) = u(h_{s1}) \quad \text{when } z > h_{s1} \tag{2.4.5}$$

The surface layer height, or better expressed the breakpoint between equations (2.4.2) and (2.4.5), is calculated for unstable and stable conditions by the following formulae:

$$h_{s1} = \begin{cases} \max\,(0.1h,\ |L|) & \text{when } L<0 \\ \max\,(200,L) & \text{when } L>0 \end{cases} \tag{2.4.6}$$

The potential temperature profile is calculated in the surface layer according to Monin-Obukhov similarity theory, by the following equation:

$$\theta(z_2)-\theta(z_1) = \frac{\theta_*}{k}\left[\ln(z_2/z_1)-\Psi_h(z_2/L)+\Psi_h(z_1/L)\right] \tag{2.4.7}$$

The stability function for heat is assumed to be equal to that for momentum and given for stable conditions (L>0) by equation (2.4.4) above.

2.5 An air mass transformation model.

To make a forecast of atmospheric boundary layer parameters, a rather detailed description is needed on the development of the meteorological conditions near the ground. In present operational 3-dimensional numerical weather models such a description can not often be introduced because of the insufficient computer capacity. Large scale weather systems, described by these models can however influence the meteorological conditions near the ground through advection.

An Air-Mass-Transformation (AMT) model has been developed by Gollvik and Omstedt (1988) for the purpuse of short-range weather forecasting of meteorological conditions in the ABL (i.e. forecast up to 12 hours). A one-dimensional boundary layer model is advected along a trajectory and influenced by fluxes at the surface. Meteorological- and physiograpic data are given from a newly developed meso-scale analysis system (Andersson et al.,1986). Trajectories and upper air meteorological data are given by the Swedish LAM-model (Undén, 1982).

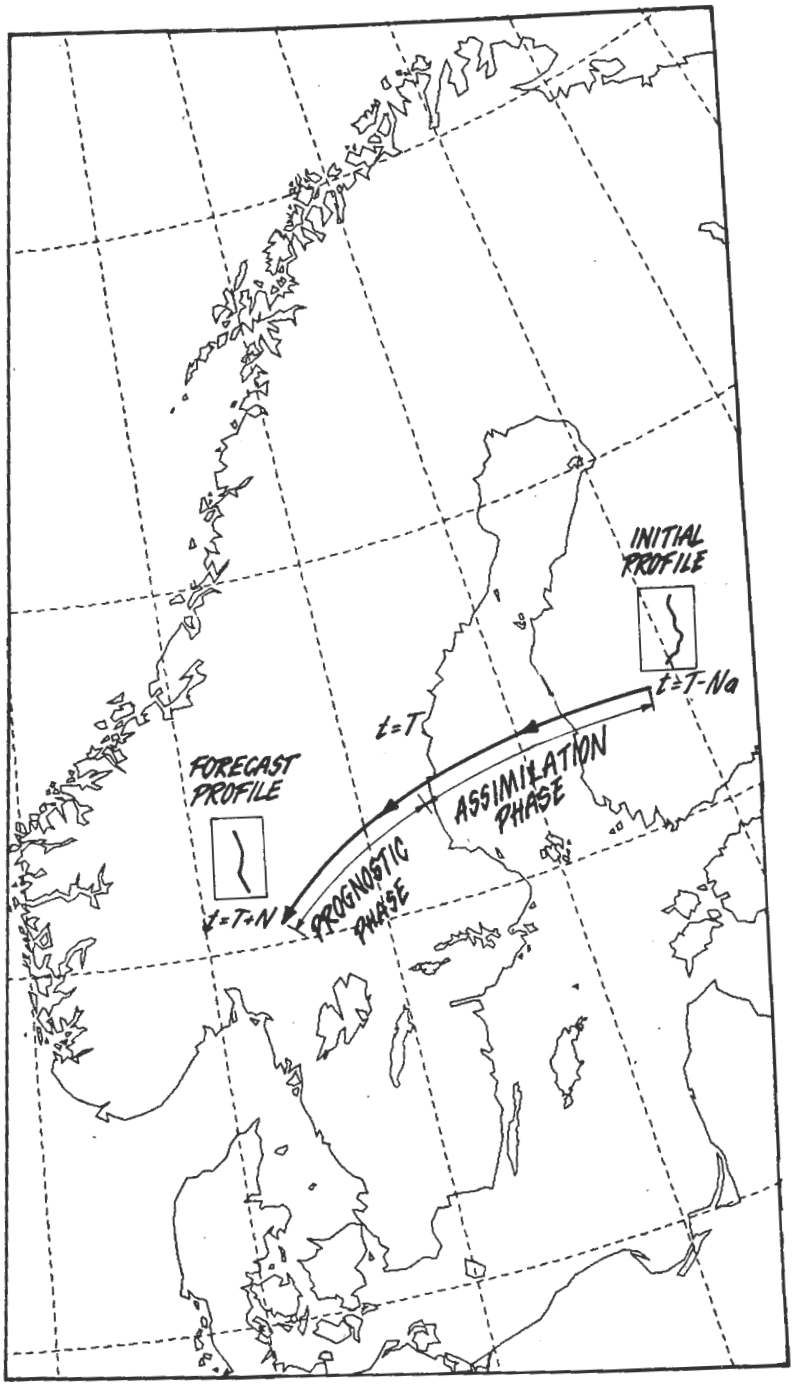

Figure 4. A schematic picture of the forecast part of the model, the so called Air-Mass-Transformation model. A one-dimensional boundary layer model is advected along a trajectory.

A general description of the AMT-model is given below.

A N-hour forecast with the AMT-model at a specific place at t=T+N hours is made in the following way (see figure 4):

1) A characteristic trajectory, for advection of a column of air, ending at t=T+N hours and originating at t=T-Na hours is calculated from the Swedish LAM-model at the lowest sigma-level (sigma=0.992), which is about 60 m above the synoptic scale LAM - orograpy.

2) By using meso-scale analyses and synoptic scale model data, a vertical profile of temperature and humidity at t=T-Na hours is estimated.

3) Along the trajectory, a one-dimensional boundary layer model is used which utilizes meso-scale information (i.e. roughness, albedo, soil moisture etc.) for the estimation of the heat-and moisture fluxes at the surface.

4) The effect of different air flow at different levels is partly taken into account, by using synoptic scale model data from LAM as forcing from the free atmosphere on the boundary layer model.

5) During the assimilation phase (from t=T-Na to t=T) analysed meso-scale information at the surface is used to estimate the fluxes of momentum, sensible- and latent heat together with analysed synoptic scale information in the free atmosphere.

6) To keep the boundary layer model as simple as possible a so called bulk model is used. The model is similar to the AMT-model developed by Reiff et al. (1984) and Driedonks et al. (1985). The basic equations are given by (2.3.1-2.3.4) above. Similar equations are used for the humidity. The large-scale vertical velocity, $\overline{w}_h$, is given by the LAM-model. For the stable boundary layer height a prognostic model developed by Nieuwstadt and Tennekes (1981) is used. They proposed that the stable boundary layer height is forced towards an equilibrium height, h_{eq}, by the following equation

$$\frac{dh}{dt} = \frac{1}{T_{sc}}(h_{eq}-h) \qquad (2.5.1)$$

where T_{sc} is a time scale given by

$$T_{sc} = -\frac{(\theta_h-\theta_s)}{d\theta_s/dt} \qquad (2.5.2)$$

($\theta_h - \theta_s$) is the temperature difference between the top and bottom of the stable boundary layer and $d\theta_s/dt$ is the rate of temperature change at the surface. Initially this time scale is small, later it may become very large.

The equilibrium height, h_{eq}, is the height of the stable boundary layer during steady-state conditions. It is calculated by the diagnostic expressions (2.3.5) and (2.3.6) given above.

Inside the boundary layer the turbulence is assumed to maintain certain relatively simple forms of vertical distributions of potential temperature and humidity. Vertical profiles are related to the bulk parameters by using so called shape functions, F(z/h), i.e.

$$\theta(z) = \theta_m + \Delta\theta F(z/h)$$
$$F(z/h) = 1-(\beta+1)(1-z/h)^{\beta} \qquad (2.5.3)$$

where β is equal to zero during unstable conditions. In the stable case the assimilation phase is used to determine the value of β in each run. Typically β varies between a value of 0.5 - 2.5. It must however be remarked that, when comparing model results with observed surface temperatures, a proper surface layer temperature profile (sec. 2.4) should be used. This profile should be matched with the temperature profile in the rest of the ABL. The fact that this is not done might lead to some error.

The surface fluxes over land are calculated using the surface energy balance method (sec. 2.2) described above. This method is generalized to different types of surfaces (i.e. grass, forest, urban) using typical albedo values, roughness values, surface wetness characteristics and different surface resistance algorithms.

In the case of a water surface, the observed sea water temperature is used and regarded as constant during a forecast. The fluxes of sensible heat and latent heat are calculated using formulae given by Burridge and Gadd (1977).

Examples of AMT-model results are shown in appendix A.

3. An air pollution model for point and area sources

An updated Gaussian air pollution model based on methods developed by Berkowicz et al. (1985) has been used in Sweden since 1985 in several different air pollution studies. Examples of such studies are given by Kindell (1987), Robertsson (1986) and Wern et al. (1987). These methods will be briefly described below.

The model is based on the well-known Gaussian plume formulation. The concentration, C, at a receptor point (x,y,z) is calculated by

$$C(x,y,z) = \frac{Q\ g_1}{u\sqrt{2\pi}\sigma_y} \frac{g_2}{\sqrt{2\pi}\sigma_z} \qquad (3.1)$$

where Q is the emission rate, u is windspeed, σ_z and σ_y are vertical and horizontal dispersion parameters respectively. The expressions g_1 and g_2 are given by:

$$g_1 = \exp(-0.5y^2/\sigma_y^2) \qquad (3.2)$$

$$g_2 = \sum_{N=-\infty}^{\infty} (\exp(-0.5(z-h_e+2Nh)^2/\sigma_z^2) + \exp(-0.5(z+h_e+2Nh)^2/\sigma_z^2)) \qquad (3.3)$$

where h_e is the effective source height and h is the boundary layer height. The effective source height is the sum of the stack height, h_s, and the final plume rise, Δh, i.e.

$$h_e = h_s + \Delta h \qquad (3.4)$$

Calculations are made in two types of coordinate systems. For calculations with a single source a polar coordinate system is used and for calculations with many sources a cartesian coordinate system is used.

3.1 Dispersion parameters

The dispersion parameters σ_z and σ_y are expressed as a sum of several contributions, each being due to one specific mechanism. Let σ denote either σ_z or σ_y then

$$\sigma^2 = \sigma^2_{turb} + \sigma^2_{buoy} + \sigma^2_{build} + \sigma^2_{area} \qquad (3.1.1)$$

where σ^2_{turb} is the contribution due to the turbulence in the ambient air, σ^2_{buoy} is the contribution due to increased internal turbulence in the buoyant plume, σ^2_{build} is the contribution due to building downwash effects and σ^2_{area} is the contribution due to the vertical and horizontal distributions of sources (used in connection with area sources).

σ^2_{turb} is decomposed in two contributions: one for convectively induced turbulence and the other for mechanical turbulence i.e.

$$\begin{cases} \sigma_z^2 = \sigma_{zc}^2 + \sigma_{zm}^2 \\ \sigma_y^2 = \sigma_{yc}^2 + \sigma_{ym}^2 \end{cases} \qquad (3.1.2)$$

The convectively generated vertical turbulent energy is described by

$$\begin{cases} \sigma_{wc}^2 = 1.54\ w_*^2 (z/h)^{2/3} & \text{for } z < 0.1\ h \\ \sigma_{wc}^2 = 0.33\ w_*^2 & \text{for } z \gg 0.1\ h \end{cases} \qquad (3.1.3)$$

and the mechanical generated vertical turbulent energy by

$$\sigma_{wm}^2 = 1.2 u_*^2 \qquad (3.1.4)$$

For convective turbulence the Lagrangian time scale is much larger than that for mechanical turbulence. It is assumed here to be "infinite". For mechanical turbulence the Lagrangian time scale is derived through a number of assumptions taking into account the fact that the length scale characterizing mechanical dispersion exhibits a strong variation with height.

The final formulae for σ_z and σ_y are given below. The convective contribution for σ_z is given by

For $h_e \geq 0.1\ h$:

$$\sigma_{zc}^2 = 0.33\ w_*^2 \left(\frac{x}{u}\right)^2$$

For $h_e < 0.1\ h$: (3.1.5)

$$\begin{cases} \sigma_{zc}^2 = 1.54\ w_*^2 (h_e/h)^{2/3} \left(\frac{x}{u}\right)^2 & \text{for } \sigma_{zc} < h_e \\ \sigma_{zc}^2 = \left(0.83 w_* h^{-1/3} \frac{x}{u} + 0.33\ h_e^{2/3}\right)^3 & \text{for } h_e \ll \sigma_{zc} < 0.1\ h \\ \sigma_{zc}^2 = \left(0.581 w_* \frac{x}{u} + 0.231\ h_e^{2/3} h^{1/3} - 0.05\ h\right)^2 & \text{for } \sigma_{zc} \geq 0.1\ h \end{cases}$$

where x is the travel distance from the source.

The mechanical contribution for σ_z is given for unstable conditions (L<0) by

$$\sigma_{zm}^2 = \sigma_{zmu}^2 = 1.2u_*^2(\frac{x}{u})^2 \exp(-0.6u_* x/uh_e) \quad \text{for } u_* x/uh_e < 1$$

$$\sigma_{zm}^2 = \sigma_{zmu}^2 = 1.2u_*^2(\frac{x}{u})^2 \exp(-0.6) \quad \text{for } u_* x/uh_e \gg 1 \qquad (3.1.6)$$

and for stable conditions (L>0) by

$$\sigma_{zm}^2 = \sigma_{zmu}^2/(1+1.1\ u_* x/uL) \qquad (3.1.7)$$

where σ_{zmu}^2 is given above and L is the Obukhov length scale.

The horizontal dispersion parameter, σ_y, is calculated basically by the following formula

$$\sigma_y = (\frac{0.25w_*^2}{1+0.9xw_*/hu} + u_*^2)^{1/2}\frac{x}{u} \qquad (3.1.8)$$

where the convective part is based on data derived from water tank experiments by Deardorff and Willis (1975).

Some modifications of the above formulae are made.

1. If the hourly sweep of the wind is larger than σ_y calculated by eq. (3.1.8), then the horizontal dispersion parameter is calculated based on the difference between two nearby wind directions.

2. Observations show that, due to meandering effects (stable, light wind conditions), the hourly averaged horizontal velocity fluctuations remain almost constant at a value of approximatively 0.5 m/s (Hanna, 1983). To take this effect into consideration u_* in equation (3.1.8) is replaced by 0.5 m/s in stable conditions when $u_* < 0.5$.

3. The effect of buoyancy is partly to increase σ as represented by the term σ_{buoy}^2 in eq (3.1.1). On the other hand, due to the greater vertical velocity of buoyant plume, such a plume is more dissociated from the ambient turbulence which tends to diminish σ. To take this effect into consideration the vertical and horizontal dispersion parameters are computed from the formulae derived above but with the travel distance x replaced by an effective travel distance X_{eff}:

$$X_{eff} = x(1-\exp(-0.15\ u/w_p)) \qquad (3.1.9)$$

where w_p is the vertical velocity of the plume.

The presence of nearby buildings can lead to an increased initial spread of the plume. Further increased dilution of the plume will result in less bouyancy and decrease the plume rise. These effects are accounted for in the model.

3.2 Plume rise and plume penetration of elevated stable layers

The procedure for plume rise calculations is based upon formulae proposed by Briggs (1975,1984) supplemented by a number of extensions. Both a so-called initial and final plume rise are computed. Near the stack, the plume rise, z', is calculated using the well-known $x^{2/3}$ dependence:

$$z' = 1.6\left(\frac{F}{u}\right)^{1/3} x^{2/3} \qquad (3.2.1)$$

where F is the buoyancy flux given by

$$F = V_s \frac{g}{T_s}(T_s - T_a) \qquad (3.2.2)$$

V_s is the volume flux, T_s, is the plume exit temperature and T_a is the ambient air temperature.

At some distance from the stack, the plume attains its final plume rise, Δh. Depending on meteorological conditions,one of several alternative processes will control the rise. One of the following methods is therefore chosen for the plume rise calculation, the choice being based on well-defined criteria:

- a method for neutral conditions:

$$\Delta h = \frac{1.3\ F}{u u_*^2}\left(1+\frac{h_s}{\Delta h}\right)^{2/3} \qquad (3.2.3)$$

where h_s is the stack heigh,

- a method for stable conditions, assuming a constant vertical temerature gradient above the stack height:

$$\Delta h = 2.6\left(\frac{F}{uS}\right)^{1/3} \qquad (3.2.4)$$

where

$$S = \frac{g}{T_a}\frac{\partial\theta}{\partial z} \qquad (3.2.5)$$

and $\partial\theta/\partial z$ is the potential temperature gradient of ambient air at the stack top,

- a method for stable conditions, assuming the presence of two layers with different vertical gradients above the stack height:

$$\Delta h = \left(\frac{2F}{u\beta'^2 S_i} + (h-h_s)\Delta h^2 - 0.5\left(\frac{h-h_s}{1.5}\right)^3\right)^{1/3} \qquad (3.2.6)$$

where β' is the entrainment parameter ($\beta'=0.4$) and S_i corresponds to eq (3.2.5) but for the potential temperature gradient in the elevated stable layer above the atmospheric boundary layer height,

- a method for convective conditions, based on the so-called break-up model:

$$\Delta h = 4.3\left(\frac{F}{u}\right)^{3/5} H_*^{-2/5} \qquad (3.2.7)$$

- a method for convective conditions, assuming partial penetration of the plume into an elevated stable layer:

$$h_e = h_s + (0.62+0.38\ P)(h-h_s) \qquad (3.2.8)$$

where P is the penetration factor and given by:

$$P=1.5-((h-h_s)/\Delta h) \quad \text{when } 0.5\leqslant((h-h_s)/\Delta h)\leqslant 1.5 \qquad (3.2.9)$$

In those cases when the plume partially penetrates above the atmospheric boundary layer an effective source strength, Q_{eff}, for penetration conditions is estimated by:

$$Q_{eff} = Q(1-P) \qquad (3.2.10)$$

4. An air pollution model for traffic sources

An air pollution model for traffic sources has been included into the model. It is based on methods developed by Johnson et al. (1973) which were improved by Bringfelt et al. (1977). The model will be briefly described below. For further details see Laurin et al. (1987).

The total air pollution concentration, C, within a street canyon is decomposed in two parts

$$C = C_b + \Delta C \qquad (4.1)$$

where C_b is the background part of the concentration coming from polluted air outside the street canyon and ΔC is the part coming from sources inside the street canyon. The background concentration, C_b, is calculated using the Gaussian air pollution model described in sec. 3 above , while ΔC is calculated by using a street canyon sub model, which in a simple way takes account of aerodynamic dispersion effects of buildings and traffic. Calculations are made for the leeward- and windward sides of a street canyon. On the leeward side of a street canyon

$$\Delta C_L = \frac{K\ Q}{(u+0.5)[(x^2+z^2)^{1/2}+L_o]} \qquad (4.2)$$

where K is an empirical constant with a typical value of 7, Q is the hourly mean emission in the street canyon, u is the roof-level wind speed, x and z are the horizontal distance and the height of the receptor relative to the centre of the traffic lane, L_o is a length scale representing the initial dispersion due to turbulence caused by traffic sources with a typical value of L_o=2 m.

On the windward side of a street canyon

$$\Delta C_w = \frac{K\ Q}{(u+0.5)W\ h_b} \qquad (4.3)$$

where W is the width of the street and h_b is the mean building height along the street.

For cases with wind directions along the street (+/- 25 deg.) the mean value of ΔC_L and ΔC_w is used i.e.

$$\Delta C_w = 0.5(\Delta C_L + \Delta C_w) \qquad (4.4)$$

If the traffic is divided into two directions these equations are solved for both directions.

Emissions of CO and NOx are calculated hourly in an emission sub-model based on information of traffic volumes, vehicle-mix, mean vehicle speeds, road types, air temperature etc. It is based on methods and values described by the Swedish Environmental Protection Board (1984).

5. Summary

This report describes an operational air pollution model developed at the Swedish Meteorological and Hydrological Institute for the purpose of predicting air pollution concentrations on a local scale i.e. a length scale of about 10 km. Predictions can be made in one or several receptor points for emissions from point, area- and traffic sources.

The physical basis for the meteorological parts of the model is provided by parameterizations of the structure of the atmospheric boundary layer. Dispersion parameters are directly related to atmospheric boundary layer parameters such as friction velocity, Obukhov length scale, convective velocity scale and boundary layer height.

Meteorological inputs are given by two meteorological preprocessors, one for climatological calculations and the other for calculations in real time or prognostic up to 12 hours.

The climatological part of the model has been used in Sweden since 1985 in several different air pollution studies.

6. Acknowledgement

I wish to thank the following colleagues at SMHI whithout whose cooperation and assistance this work could not have been performed: Björn Bringfelt, Sture Ring, Christina Lindgren, Gunnar Pettersson, Sven Kindell, Lennart Robertsson, Lennart Wern, Stefan Gollvik. Special thanks are due to the staff of the Danish Air Pollution Laboratory for useful discussions and helpfulness during my visit there. I also wish to thank Jose Melgarejo for the review of this report.

7. REFERENCES

Anderson,E.,Gustavsson,N.,Meuller,L. and Omstedt,G.,1986. Development of meso-scale analysis schemes for nowcasting and very short-range forcasting. SMHI-report, PROMIS nr 1.

Bäckström,M.,Lindgren,C. och Omstedt,G.,1984. Bruksanvisning för en operationell luftföroreningsmodell. FOU-notis (SMHI).

Berkowicz,R. and Prahm,L.P.,1982. Sensibel heat flux estimated from routine meteorological data by the resistance method. J. Appl. Met. 21, 1845-1864.

Berkowicz,R.,Olesen,H.R.and Torp,U.,1985. The Danish Gaussian air pollution model (OML): Description, test and sensitivity analysis in view of regulatory applications. Proceedings of the 15th International Technical Meeting on Air Pollution Modeling and its Applications - St. Louise, USA, April 16-19,1985.

Briggs,G.A.,1975. Plume rise predictions. In Lectures on air pollution and environmental impact analyses, American Meteorological Society, BOSTON, MA.

Briggs,G.A.,1984. Plume rise and buoyancy effects. In Atmospheric science and power production, Atmospheric Turbulence and Diffusion Laboratory, NOAA, Oak Ridge, TN.

Bringfelt,B. och Laurin,S.,1977. Bilavgaser i gatumiljö - modell och modelltest. Statens Naturvårdsverk, SNV PM 891 och 1393.

Burridge,D.M., and Gadd,A.J.,1977. The meteorological office operational 10-level numerical weather prediction model. Sci. Paper No.34, Meteor. Office, London Road, Bracknell, Berkshire RG12 2SZ, England, 1-39.

Deardorff,J.W. and Willis,G.E.,1975. A parameterization of diffusion into mixed layer. J. Appl. Meteor.,14, 1451-1458.

Dyer,A.J.,1974. A review of flux-profile relationships. Boundary-Layer Meteorol.,7,363-372.

Driedonks,A.G.M.,1982.Models and observations of the growth of the atmospheric boudary layer. Boundary Layer Meteorology, 23,283-306.

Driedonks,A.G.M.,J.Reiff and Holtslag,A.A.M.,1985. Mesoscale results of an Air-Mass Transformation Model. Contribution to Atmospheric Physics, 58, 361-379.

Gollvik,S., and Omstedt,G.,1988. An air mass transformation model for short-range weather forcasting. SMHI-report.

Hanna,S.R.,1983. Lateral turbulence intensity and plume meandering during stable conditions. J. Clim. Appl. Met., 22, 1424-1430.

Holtslag,A.A.M.,1984. Estimates of diabatic wind speed profiles from near surface weather observations. Boundary-Layer Meteorol.,29, 225-250.

Holtslag,A.A.M. and de Bruin, H.A.R.,1988. Applied modelling of the nighttime surface energy balance over land. J. App. Met.,22,689-704.

Johnson,W.B.,Ludwig,F.L.,Dabberdt,W.F. and Allen,R.J.,1973. An urban diffusion simulation model for carbon monoxide. J. of the Air Pollution Control Association. Vol. 23, No.6, 490-498.

Kindell,S.,1987. Luften i Nässjö. SMHI-rapport nr. 57.

Laurin,S. och Omstedt,G.,1987. En modell för beräkningar av bilavgaser i gatumiljö (SMHI).

Nieuwstadt,F.T.M. and Tennekes,H.,1981. A rate equation for the nocturnal boundary-layer height. J. Atmos. Sci., 38, 1418-1428.

Nieuwstadt,F.T.M.,1984.Some aspects of the turbulent stable boundary layer. Boundary-Layer Meteorol.,30, 31-55.

Nielsen,L.B.,Prahm,L.P.,Berkowicz,R.and Conradson,K.,1981. Net incoming radiation estimated from hourly global radiation and/or cloud observations. J. Climat. 1,255.

Olesen,H.R.,Jensen,A.B. and Brown,N.,1985. An operational procedure for mixing height estimation. MST LUFT-A 96. National Agency of Environmental Protection, Air pollution Laboratory, Riso, DK-4000, Roskilde, Denmark.

Reiff,J.,Blaauboer,D.,De Bruin,H.A.R.,Van Ulden,A.P. and Cats,G., 1984. An air mass transformation model for short-range weather forecasting. Monthly Weather Review, vol.112, 393-412.

Robertsson,L.,1986. Koncentrations- och depositions-beräkningar för Halmstads avfallsförbränningsanläggning vid Kristinehed. SMHI-rapport nr. 10.

Swedish Environmental Protection Board,1984. Beräkning av avgashalter vid gator och vägar. SNV, meddelande nr 8/1984.

Tennekes,H.,1973.A model for the dynamics of the inversion above a convective layer. J. Atmos. Sci.,30, 558-567.

Tennekes,H. and Driedonks,A.G.M.,1981.Basic entrainment equations for the atmospheric boundary layer. Boundary-Layer Meteorol.,20, 515-531.

Undén,P.,1982. The Swedish Limited Area Model. SMHI Rep., Met. and Clim., RMK 35,33.

Van Ulden,A.P. and Holtslag,A.A.M.,1985. Estimation of atmospheric boundary layer parameters for diffusion applications. Journal of Climate and Applied Meteorology, Vol.24, No. 11, 1196-1207.

Wern,L.,Laurin,S. och Omstedt,G.,1987. Luften i Halmstad. SMHI-rapport nr. 11.

Zilitinkevich,S.S.,1972. On the determination of the height of the Ekman boundary layer. Boundary-Layer Meteorol. ,3, 141-145.

Examples of AMT-model results APPENDIX A

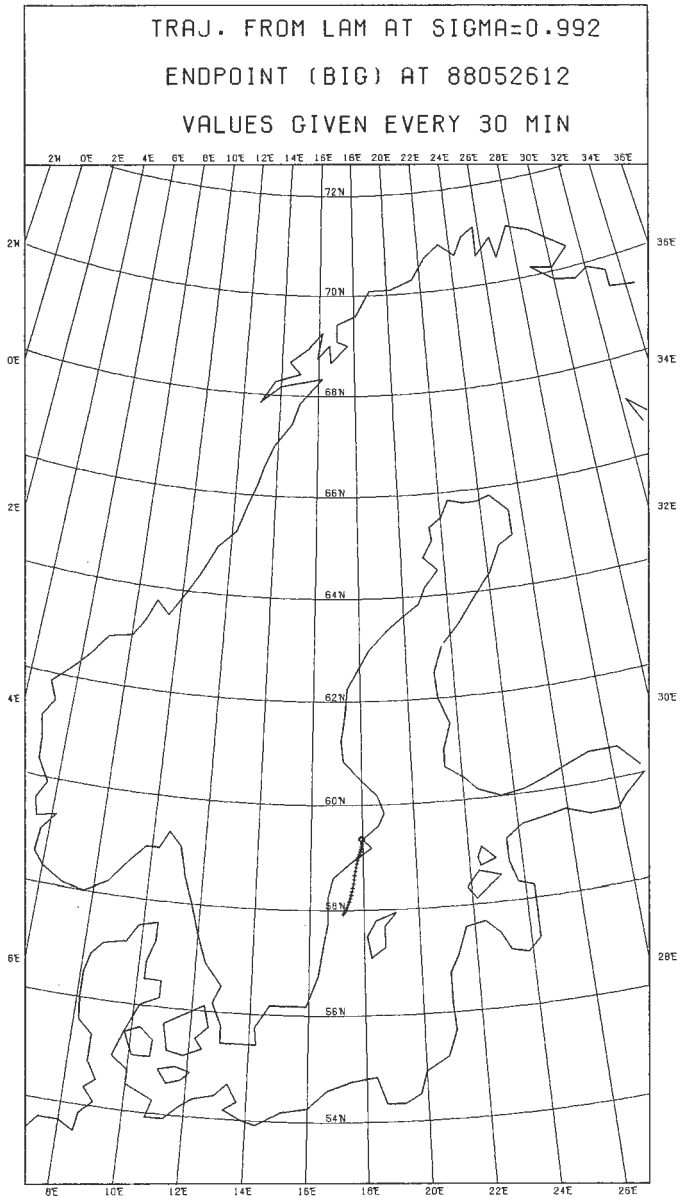

Figure A1.

Results from a 12-hours forecast. The forecast results (left bottom) are compared with the sounding (right bottom) at Bromma airport 880526 12 UTC

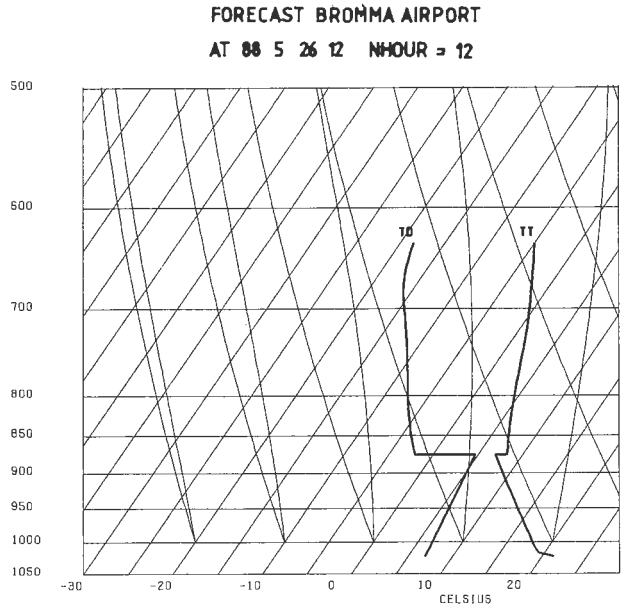

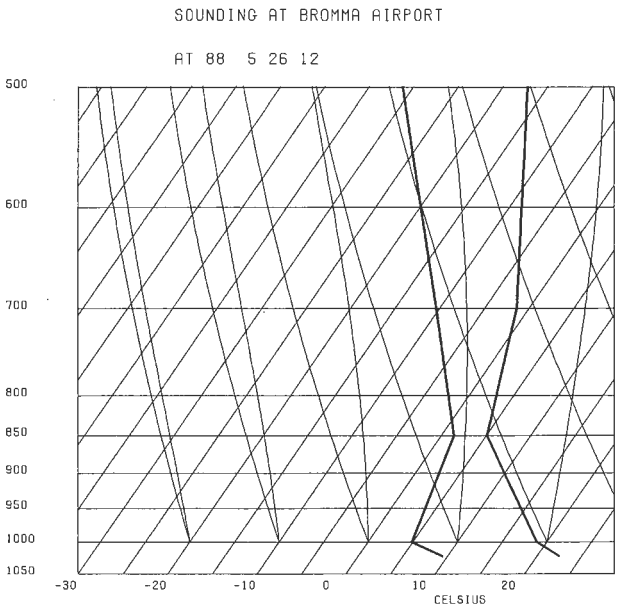

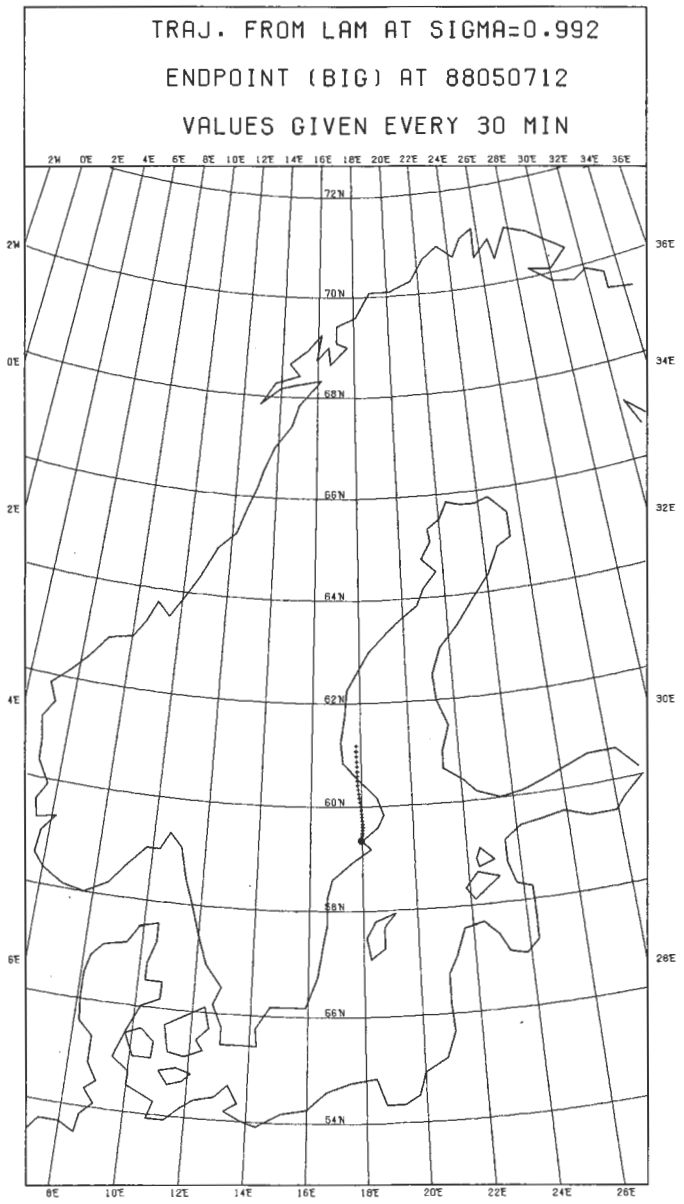

Figure A2.

Results from a 6-hours forecast. The forecast results (left bottom) are compared with the sounding (right bottom) at Bromma airport 880507 12 UTC.

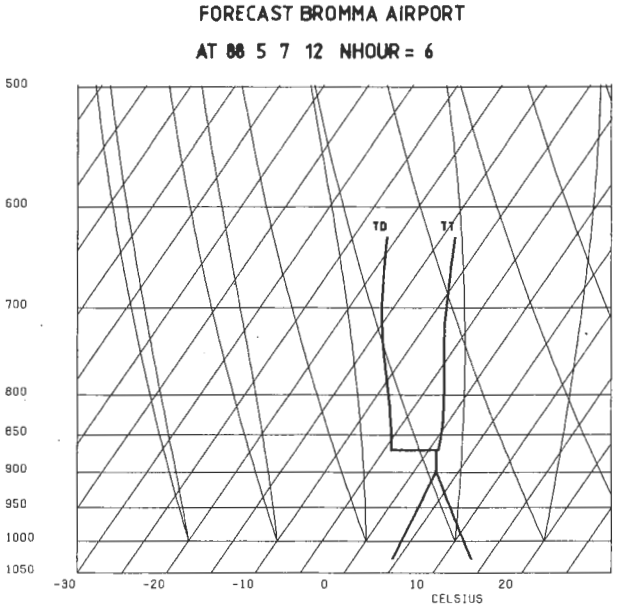

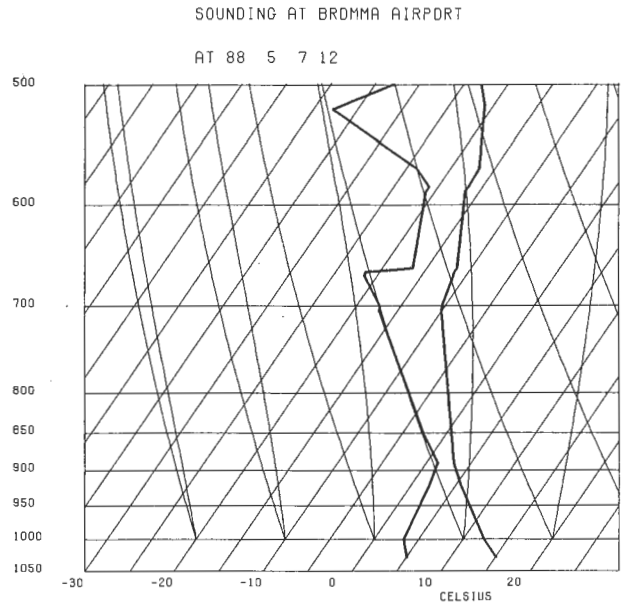

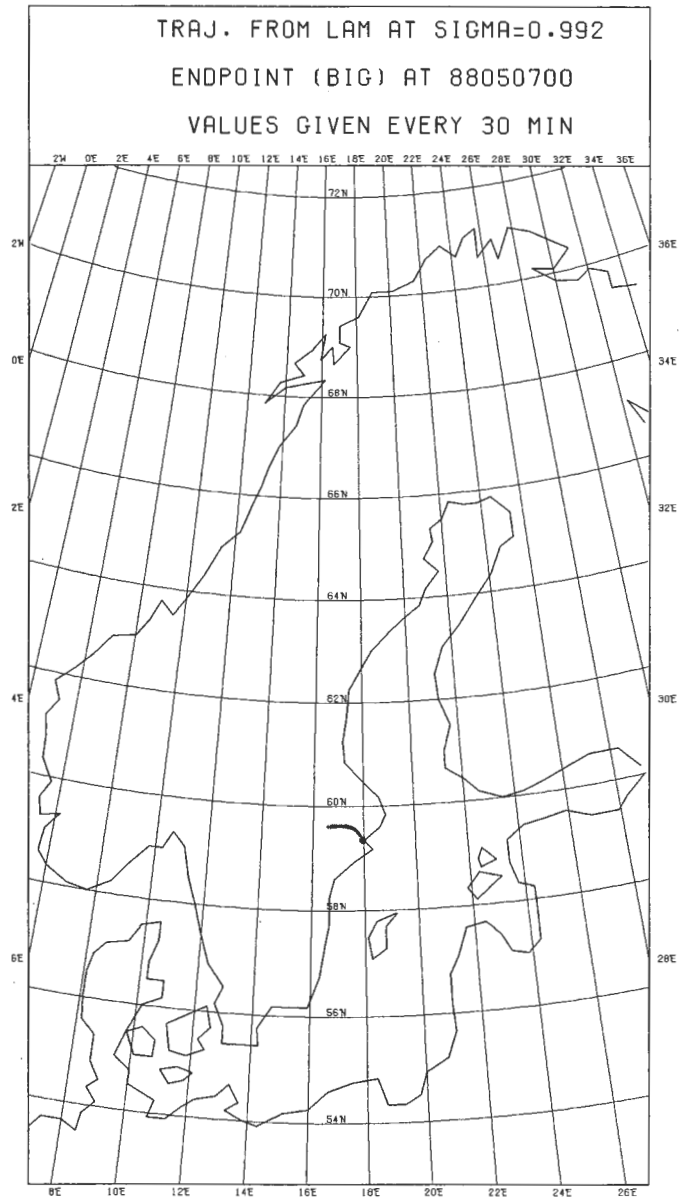

Figure A3.

Results from a 6-hours forecast. The forecast results (left bottom) are compared with the sounding (right bottom) at Bromma airport 880507 00 UTC.

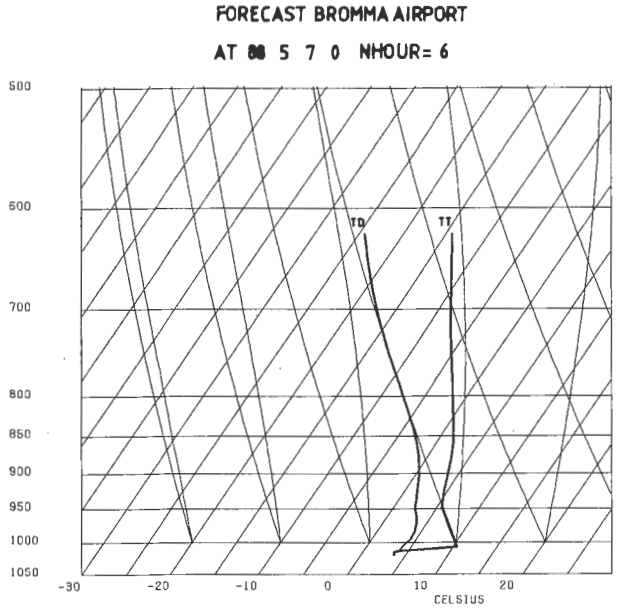

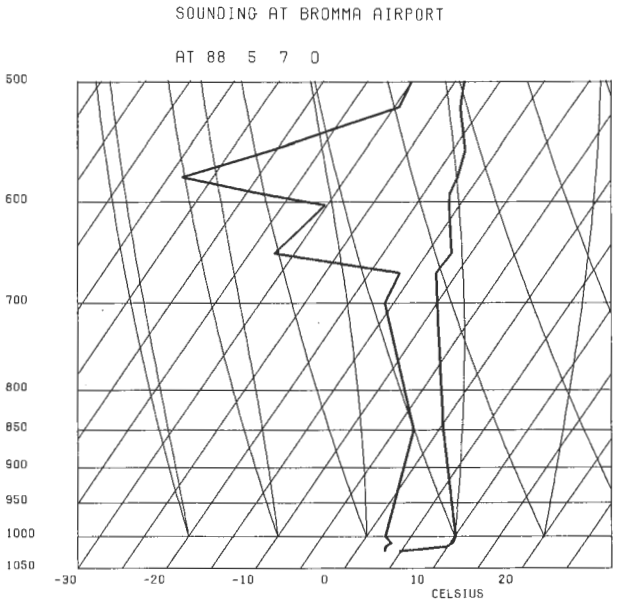

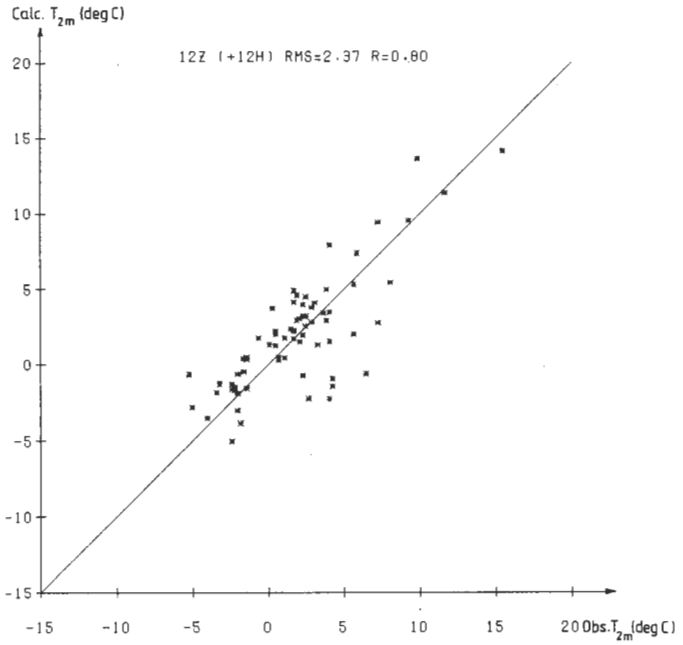

Figure A4.

Comparison between observed and calculated (12-hours forecast) T_2m (deg C) at Bromma airport at 12 UTC during winter 1988. RMS is root-mean-square error and R is correlation coefficient.

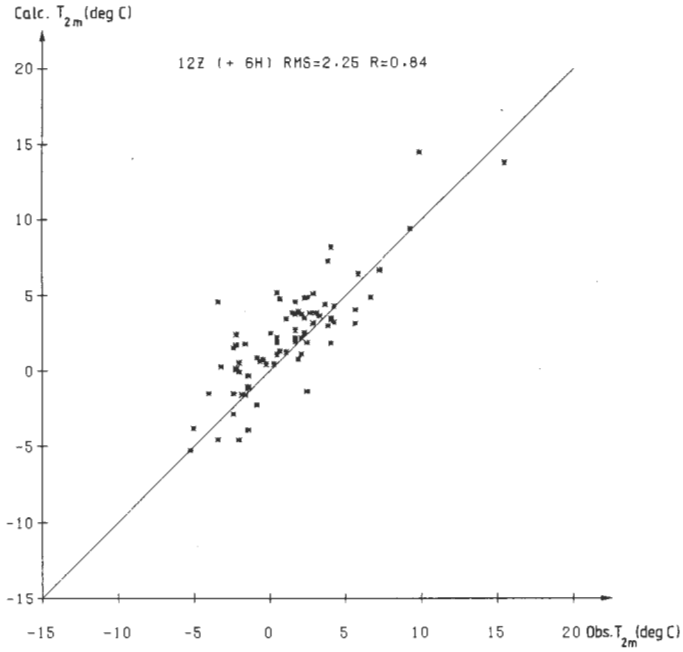

Figure A5.

Comparison between observed and calculated (6 hours forecast) T_2m (deg C) at Bromma airport at 12 UTC during winter 1988. RMS is root-mean-square error and R is correlation coefficient.

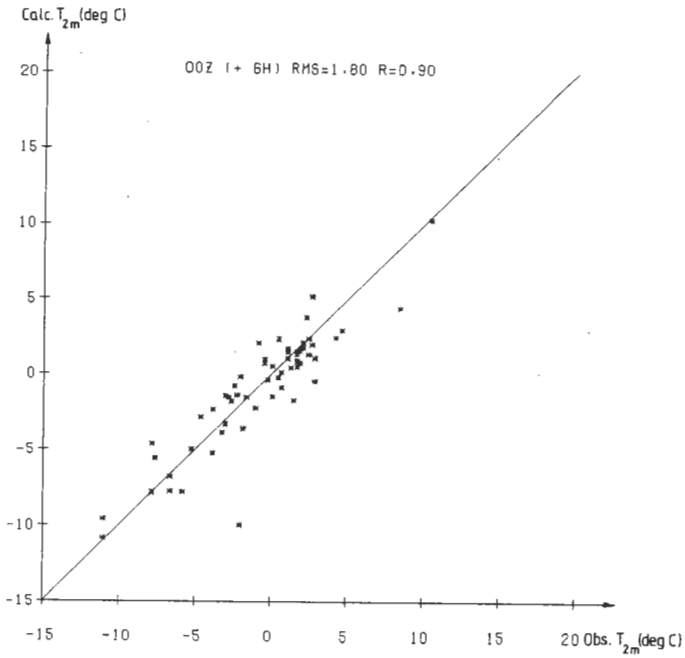

Figure A6.

Comparison between observed and calculated (6-hours forecast) T_2m (deg C) at Bromma airport at 00 UTC during winter 1988. RMS is root-mean-square error and R is correlation coefficient.

SMHI Rapporter, METEOROLOGI OCH KLIMATOLOGI (RMK)

Nr 1 Thompson, T, Udin, I, and Omstedt, A
Sea surface temperatures in waters surrounding Sweden
Stockholm 1974

Nr 2 Bodin, S
Development on an unsteady atmospheric boundary layer model.
Stockholm 1974

Nr 3 Moen, L
A multi-level quasi-geostrophic model for short range weather predictions
Norrköping 1975

Nr 4 Holmström, I
Optimization of atmospheric models
Norrköping 1976

Nr 5 Collins, W G
A parameterization model for calculation of vertical fluxes of momentum due to terrain induced gravity waves
Norrköping 1976

Nr 6 Nyberg, A
On transport of sulphur over the North Atlantic
Norrköping 1976

Nr 7 Lundqvist, J-E, and Udin, I
Ice accretion on ships with special emphasis on Baltic conditions
Norrköping 1977

Nr 8 Eriksson, B
Den dagliga och årliga variationen av temperatur, fuktighet och vindhastighet vid några orter i Sverige
Norrköping 1977

Nr 9 Holmström, I, and Stokes, J
Statistical forecasting of sea level changes in the Baltic
Norrköping 1978

Nr 10 Omstedt, A, and Sahlberg, J
Some results from a joint Swedish-Finnish sea ice experiment, March, 1977
Norrköping 1978

Nr 11 Haag, T
Byggnadsindustrins väderberoende, seminarieuppsats i företagsekonomi, B-nivå
Norrköping 1978

Nr 12 Eriksson, B
Vegetationsperioden i Sverige beräknad från temperaturobservationer
Norrköping 1978

Nr 13 Bodin, S
En numerisk prognosmodell för det atmosfäriska gränsskiktet grundad på den turbulenta energiekvationen
Norrköping 1979

Nr 14 Eriksson, B
Temperaturfluktuationer under senaste 100 åren
Norrköping 1979

Nr 15 Udin, I, och Mattisson, I
Havsis- och snöinformation ur datorbearbetade satellitdata - en modellstudie
Norrköping 1979

Nr 16 Eriksson, B
Statistisk analys av nederbördsdata. Del I. Arealnederbörd
Norrköping 1979

Nr 17 Eriksson, B
Statistisk analys av nederbördsdata. Del II. Frekvensanalys av månadsnederbörd
Norrköping 1980

Nr 18 Eriksson, B
Årsmedelvärden (1931-60) av nederbörd, avdunstning och avrinning
Norrköping 1980

Nr 19 Omstedt, A
A sensitivity analysis of steady, free floating ice
Norrköping 1980

Nr 20 Persson, C och Omstedt, G
En modell för beräkning av luftföroreningars spridning och deposition på mesoskala
Norrköping 1980

Nr 21 Jansson, D
Studier av temperaturinversioner och vertikal vindskjuvning vid Sundsvall-Härnösands flygplats
Norrköping 1980

Nr 22 Sahlberg, J and Törnevik, H
A study of large scale cooling in the Bay of Bothnia
Norrköping 1980

Nr 23 Ericson, K and Hårsmar, P-O
Boundary layer measurements at Klockrike. Oct. 1977
Norrköping 1980

Nr 24 Bringfelt, B
A comparison of forest evapotranspiration determined by some independent methods
Norrköping 1980

Nr 25 Bodin, S and Fredriksson, U
Uncertainty in wind forecasting for wind power networks
Norrköping 1980

Nr 26 Eriksson, B
Graddagsstatistik för Sverige
Norrköping 1980

Nr 27 Eriksson, B
Statistisk analys av nederbördsdata. Del III. 200-åriga nederbördsserier
Norrköping 1981

Nr 28 Eriksson, B
Den "potentiella" evapotranspirationen i Sverige
Norrköping 1981

Nr 29 Pershagen, H
Maximisnödjup i Sverige (perioden 1905-70)
Norrköping 1981

Nr 30 Lönnqvist, O
Nederbördsstatistik med praktiska tillämpningar
(Precipitation statistics with practical applications)
Norrköping 1981

Nr 31 Melgarejo, J W
Similarity theory and resistance laws for the atmospheric boundary layer
Norrköping 1981

Nr 32 Liljas, E
Analys av moln och nederbörd genom automatisk klassning av AVHRR data
Norrköping 1981

Nr 33 Ericson, K
Atmospheric Boundary layer Field Experiment in Sweden 1980, GOTEX II, part I
Norrköping 1982

Nr 34 Schoeffler, P
Dissipation, dispersion and stability of numerical schemes for advection and diffusion
Norrköping 1982

Nr 35 Undén, P
The Swedish Limited Area Model (LAM). Part A. Formulation
Norrköping 1982

Nr 36 Bringfelt, B
A forest evapotranspiration model using synoptic data
Norrköping 1982

Nr 37 Omstedt, G
Spridning av luftförorening från skorsten i konvektiva gränsskikt
Norrköping 1982

Nr 38 Törnevik, H
An aerobiological model for operational forecasts of pollen concentration in th air
Norrköping 1982

Nr 39 Eriksson, B
Data rörande Sveriges temperaturklimat
Norrköping 1982

Nr 40 Omstedt, G
An operational air pollution model using routine meteorological data
Norrköping 1984

Nr 41 Persson, Christer, and Funkquist, Lennart
Local scale plume model for nitrogen oxides.
Model description.
Norrköping 1984

Nr 42 Gollvik, Stefan
Estimation of orographic precipitation by dynamical interpretation of synoptic model data.
Norrköping 1984

Nr 43 Lönnqvist, Olov
Congression - A fast regression technique with a great number of functions of all predictors.
Norrköping 1984

Nr 44 Laurin, Sten
Population exposure to So and NO_x from different sources in Stockholm.
Norrköping 1984

Nr 45 Svensson, Jan
Remote sensing of atmospheric temperature profiles by TIROS Operational Vertical Sounder.
Norrköping 1985

Nr 46 Eriksson, Bertil
Nederbörds- och humiditetsklimat i Sverige under vegetationsperioden.
Norrköping 1986

Nr 47 Taesler, Roger
Köldperioder av olika längd och förekomst.
Norrköping 1986

Nr 48 Wu Zengmao
Numerical study of lake-land breeze over Lake Vättern, Sweden.
Norrköping 1986

Nr 49 Wu Zengmao
Numerical analysis of initialization procedure in a two-dimensional lake breeze model.
Norrköping 1986

Nr 50 Persson, Christer
Local scale plume model for nitrogen oxides. Verification.
Norrköping 1986

Nr 51 Melgarejo, José W.
An analytical model of the boundary layer above sloping terrain with an application to observations in Antarctica
Norrköping 1986

Nr 52 Bringfelt, Björn
Test of a forest evapotranspiration model
Norrköping 1986

Nr 53 Josefsson, Weine
Solar ultraviolet radiation in Sweden
Norrköping 1986

Nr 54 Dahlström, Bengt
Determination of areal precipitation for the Baltic sea
Norrköping 1986

Nr 55 Persson, Christer (SMHI), Rodhe, Henning (MISU), De Geer, Lars-Erik (FOA)
The Chernobyl accident - A meteorological analysis of how radionucleides reached Sweden.
Norrköping 1986

Nr 56 Persson, Christer, Robertsson, Lennart (SMHI), Grennfelt, Peringe, Kindbom, Karin, Lövblad, Gun, och Svanberg, Per-Arne (IVL)
Luftföroreningsepisoden över södra Sverige 2 - 4 februari 1987
Norrköping 1987

Nr 57 Omstedt, Gunnar
An operational air pollution model
Norrköping 1988

SMHI
Swedish meteorological and hydrological institute
S-60176 Norrköping, Sweden. Tel. +46 11 15 80 00. Telex 644 00 smhi s.

ISSN 0347-2116